



ARTICLE

PPAR α agonist fenofibrate relieves acquired resistance to gefitinib in non-small cell lung cancer by promoting apoptosis via PPAR α /AMPK/AKT/FoxO1 pathway

Mei-sa Wang¹, Qiu-shuang Han¹, Zhi-rong Jia¹, Chuan-sheng Chen¹, Chen Qiao², Qian-qian Liu¹, Ya-meng Zhang¹, Kai-wei Wang¹, Jie Wang^{1,3}, Kang Xiao¹ and Xuan-sheng Ding^{1,2}

Recent studies show that intracellular accumulation of cholesterol leads to acquired resistance to gefitinib in non-small cell lung cancer (NSCLC) cells. In this study we investigated how to regulate the cholesterol levels in gefitinib-resistant NSCLC cells. We showed that intracellular cholesterol levels in gefitinib-resistant cell lines (PC-9/GR, H1975, H1650, and A549) were significantly higher than that in gefitinib-sensitive cell line (PC-9). Treatment with gefitinib (5 μ M) significantly increased intracellular cholesterol levels in PC-9/GR, H1975, and H1650 cells. Gefitinib treatment downregulated the expression of PPAR α , LXRA, and ABCA1, leading to dysregulation of cholesterol efflux pathway. We found that a lipid-lowering drug fenofibrate (20, 40 μ M) dose-dependently increased the expression of PPAR α , LXRA, and ABCA1, decreased the intracellular cholesterol levels, and enhanced the antiproliferative effects of gefitinib in PC-9/GR, H1975, and H1650 cells. We revealed that fenofibrate increased the gefitinib-induced apoptosis via regulating the key proteins involved in the intrinsic apoptosis pathway. In PC-9/GR, H1975 and H1650 cells, fenofibrate dose-dependently increased the expression of AMPK, FoxO1, and decreased the expression of AKT, which were remarkably weakened by knockdown of PPAR α . In PC-9/GR cell xenograft mice, combined administration of gefitinib (25 mg \cdot kg⁻¹ \cdot d⁻¹) and fenofibrate (100 mg \cdot kg⁻¹ \cdot d⁻¹) caused remarkable inhibition on tumor growth as compared to treatment with either drug alone. All the results suggest that fenofibrate relieves acquired resistance to gefitinib in NSCLC by promoting apoptosis via regulating PPAR α /AMPK/AKT/FoxO1 pathway. We propose that combination of gefitinib and fenofibrate is a potential strategy for overcoming the gefitinib resistance in NSCLC.

Keywords: non-small-cell lung cancer; gefitinib; acquired resistance; cholesterol; fenofibrate; apoptosis; PPAR α /AMPK/AKT/FoxO1 pathway

Acta Pharmacologica Sinica (2022) 43:167–176; <https://doi.org/10.1038/s41401-021-00638-z>

INTRODUCTION

Lung cancer, the most common cancer, has the highest incidence and substantially mortality among all malignancies [1]. Histologically, lung cancer is divided into non-small-cell lung cancer (NSCLC) and small-cell lung cancer (SCLC), of which NSCLC comprises more than 80% [2]. Thirty percent of patients with NSCLC harbor active epidermal growth factor receptor (EGFR) mutations and respond well to tyrosine kinase inhibitors (TKIs) [3]. Gefitinib is a commonly used TKI for the clinical treatment of NSCLC [3]. However, acquired resistance to gefitinib is a huge obstacle for gefitinib treatment. Most patients with NSCLC exhibit drug resistance and poor prognosis after 10–16 months of gefitinib treatment [4, 5]. The base molecular mechanisms of acquired gefitinib resistance include the T790M mutation in exon 20 of EGFR, MET, and HER2 amplification and the loss of PTEN [6]. However, the underlying pathways leading to these molecular mechanisms of acquired gefitinib resistance remain unclear, so it is necessary to explore feasible methods to solve this problem.

Differences in lipid metabolism between cancer and normal cells are now gaining recognition as hallmarks of cancer [7]. Cholesterol is a significant component of lipid metabolism, and reprogramming of this metabolic pathway in cancer is known to be important for cell proliferation and drug resistance [8, 9]. In addition to maintaining the stability of the cell membrane, cholesterol is also an intrinsic component for lipid rafts, which can activate various membrane-related cellular signaling pathway [8, 9]. A previous study revealed that high cholesterol levels in lipid rafts promote gefitinib resistance via EGFR binding affinity and downstream signaling pathways in NSCLC cells [10]. The dependence of NSCLC cells on dysregulated cholesterol metabolism shows that key proteins in this process are potential therapeutic targets [11]. Multiple pathways were found to increase the intracellular cholesterol level in cancer cells [12]. A net increase in cholesterol levels in cancer cells could be a result of dysregulation in synthesis, uptake or efflux pathways [13]. These include upregulation of 3-hydroxy-3-methylglutaryl CoA reductase

¹School of Basic Medicine and Clinical Pharmacy, China Pharmaceutical University, Nanjing 210009, China; ²Precision Medicine Laboratory, School of Basic Medicine and Clinical Pharmacy, China Pharmaceutical University, Nanjing 210009, China and ³Department of Pharmacy, the First Affiliated Hospital of Xinjiang Medical University, Urumqi 830054, China

Correspondence: Xuan-sheng Ding (dxs0162@sina.com)

Received: 25 September 2020 Accepted: 3 March 2021

Published online: 26 March 2021

(HMGCR) protein expression, increased uptake of extracellular cholesterol by low-density lipoprotein receptor and decreased activity of ATP binding cassette transporter A1 (ABCA1) to prevent the efflux of cholesterol. Peroxisome proliferator-activated receptor α (PPAR α), a member of the peroxisome proliferator-activated receptor (PPAR) family, is a key regulator of cholesterol metabolism in human cells [14]. Most cells and tissues lack the ability to metabolize cholesterol and depend on efflux pathways to maintain cellular cholesterol homeostasis [13]. In cells, PPAR α can trigger the transcription of liver X receptors (LXR α) and regulate ABCA1 expression to influence cholesterol efflux, and intracellular cholesterol is increased by disordered PPAR α gene expression [15].

Fenofibrate, a PPAR α agonist, belongs to the fibrate class of lipid-lowering drugs [16]. It has been used in the treatment of hypercholesterolemia and hyperlipidemia by lowering total cholesterol and triglyceride levels [17]. Recent studies have revealed that fenofibrate has potential as an antitumor drug. Fenofibrate could inhibit the cell proliferation of lung cancer, breast cancer, glioma, liver cancer and prostate cancer by inducing cell cycle arrest and apoptosis [18]. Furthermore, fenofibrate could enhance chemosensitivity in cancers, for instance, by modulating the apoptotic pathway to increase the sensitivity of breast cancer to paclitaxel [19] and reducing the effective doses of docetaxel by interfering with drug resistance in prostate cancer [20]. However, no studies have reported how fenofibrate sensitizes NSCLC cells to EGFR-TKIs.

In the present research, we propose a hypothesis that fenofibrate could promote the sensitization of cells to gefitinib treatment by activating the PPAR α /LXR α /ABCA1 axis to reduce intracellular cholesterol levels. Furthermore, fenofibrate could increase gefitinib-induced apoptosis by influencing the AMPK/AKT/FoxO1 pathway in a PPAR α -dependent manner. Our study demonstrates that the combination of gefitinib and fenofibrate is a potential treatment strategy for gefitinib resistance in NSCLC.

MATERIALS AND METHODS

Cell culture and reagents

The human NSCLC cell lines A549, H1975, and H1650 were purchased from the Cell Bank of the Shanghai Academy of Life Sciences (Shanghai, China), and PC-9 and PC-9/GR cell lines were gifts from Dr Cai-cun Zhou (Shanghai Pulmonary Hospital, Shanghai, China). All cells were cultured in RPMI-1640 (KeyGen BioTECH, Nanjing, China) supplemented with 10% FBS (Gibco, Gaithersburg, MD, USA) and penicillin/streptomycin/amphotericin B sterile solution (Solarbio, Beijing, China) and maintained at 37 °C in a humidified cell incubator with 5% CO₂. Cells were grown to 70%–80% confluence, harvested with trypsin, and suspended to the cell density required for each assay.

Reagents and chemicals

The reagents used in this study were purchased as follows. Gefitinib was purchased from Selleck (Shanghai, China), and fenofibrate was purchased from MedChemExpress (New Jersey, USA). SC79 was purchased from MedChemExpress (New Jersey, USA). Before they were added to cell cultures, all drugs were prepared in dimethyl sulfoxide for in vitro analyses.

Amplex® red cholesterol assay

Samples were collected to determine intracellular cholesterol levels by using the Amplex® Red Cholesterol Assay Kit (Invitrogen, Carlsbad, CA, USA) according to the manufacturer's instructions. Cells were lysed in RIPA buffer (KeyGENBioTECH, Nanjing, China) with 1 mM PMSF (KeyGENBioTECH, Nanjing, China) and 1× cocktails (KeyGENBioTECH, Nanjing, China), and a BCA protein assay (Beyotime Biotechnology, Shanghai, China) was performed. The extracts or the medium was diluted with 1× reaction buffer,

and 50 μ L of Amplex Red reagent was added to 50 μ L samples in 96-well opaque plates. The reactions were incubated for 30 min at 37 °C in the dark. Fluorescence was measured by a fluorescence microplate reader (Thermo Fisher Scientific, Waltham, MA, USA) with an excitation wavelength at 550 nm and an emission wavelength at 590 nm. The cholesterol levels were calculated from the standard curve.

Cell viability assay

Cell viability was determined by the CCK-8 assay (APExBIO, Houston, TX, USA). Cells in the logarithmic growth phase were harvested and plated in 96-well plates at a concentration of 5×10^3 cells per well and incubated overnight. Following cell adherence, various gefitinib concentrations (0, 0.9375, 1.875, 3.75, 15.30, and 60 μ M) with or without different concentrations of fenofibrate (20 and 40 μ M) were added, cells were incubated for 48 h. According to the specification, CCK-8 reagents were added to each well, and the plates were incubated for an additional 4 h at 37 °C. The absorbance was measured at 450 nm with a microplate reader. The results are expressed as the inhibition rate of cells compared to the normal controls, which is shown as the mean \pm standard deviation (SD) ($n=6$ for each group). The combination index (CI) values were calculated using CompuSyn software (ComboSyn, Inc., NJ, USA). Each experiment was performed in triplicate.

Colony formation assay

Cells were seeded at a density of 200 cells per well in six-well plates. After incubation for 24 h, the cells were treated with gefitinib (5 μ M) alone, fenofibrate (20, 40 μ M) alone or both drugs diluted with medium to the appropriate concentrations, and the medium was replaced every 3 d. After two weeks, cells were stained with 0.1% crystal violet (KeyGENBioTECH, Nanjing, China). Colonies with a diameter greater than 1 mm were counted, and each experiment was repeated three times.

Quantitative real-time PCR

Total RNA of cells treated with gefitinib was isolated from cell lines using TRIzol (Invitrogen, Carlsbad, CA, USA). According to the manufacturer's instructions, qualified RNA was used for cDNA synthesis with HiScript® III RT SuperMix (Vazyme, Nanjing, China). Quantitative PCR was performed using ChamQ™ SYBR® qPCR Master Mix (Vazyme, Nanjing, China). GAPDH was used as an internal control to normalize the amount of total RNA in each sample. The primer sequences were as follows: GAPDH forward, 5'-ACCACAGTCCATGCCATCAC-3' and reverse, 5'-TCCACCACCCTGTGCTGTGA-3'; and PPAR α forward, 5'-AGGCTATCATTACGGAGTC-3' and reverse, 5'-GTCGCACCTGTCATACAC-3'. The results were analyzed with the $\Delta\Delta$ Ct method.

Western blot analysis

Cells were lysed with RIPA buffer (KeyGENBioTECH, Nanjing, China) containing 1 mM PMSF and protease inhibitor cocktail and incubated on ice. Following centrifugation at 12,000 $\times g$ for 15 min at 4 °C, proteins in the supernatants were quantified by a BCA Protein Assay Kit. Equal amounts of protein were separated in SDS-PAGE gels and transferred to PVDF membranes. Membranes were blocked in 10% milk for 2 h and then incubated overnight (4 °C) with antibodies against GAPDH (Proteintech, Wuhan, China), PPAR α (Proteintech, Wuhan, China), β -actin (Proteintech, Wuhan, China), LXR α (HUABIO, Hangzhou, China), ABCA1 (HUABIO, Hangzhou, China), Bcl-2 (Cell Signaling Technology, Boston, MA, USA), Caspase-3 (Cell Signaling Technology, Boston, MA, USA), Caspase-7 (Cell Signaling Technology, Boston, MA, USA), Caspase-8 (Cell Signaling Technology, Boston, MA, USA), Caspase-9 (Cell Signaling Technology, Boston, MA, USA), Bax (Cell Signaling Technology, Boston, MA, USA), AKT (Cell Signaling Technology, Boston, MA, USA), p-AKT (Cell Signaling Technology, Boston, MA, USA), AMPK (Cell

Signaling Technology, Boston, MA, USA), p-AMPK (Cell Signaling Technology, Boston, MA, USA), Foxo1 (Cell Signaling Technology, Boston, MA, USA), and p-Foxo1 (Cell Signaling Technology, Boston, MA, USA). After being washed in TBS-T, membranes were incubated with the corresponding horseradish peroxidase (HRP)-conjugated secondary antibody for 1 h at room temperature. The blots were visualized by ECL detection. Protein expression was quantified by ImageJ. Three individual experiments were repeated.

siRNA transfection

Small-interfering RNA (siRNA) duplexes for PPAR α and AMPK were designed and synthesized by TranSheep Bio (Shanghai, China). Cells were transfected with siRNA or negative control using Lipofectamine 2000 (Invitrogen, Carlsbad, CA, USA) according to the manufacturer's instructions. For transfection, cells were seeded in six-well plates at 60%–70% confluency, and then siRNA (5 nM) was delivered into the cells using Lipofectamine 2000 in serum-free Opti-MEM media. After 6 h, the medium was replaced with RPMI-1640 containing 10% FBS for continuous culture.

Apoptosis detection

Cells were seeded in six-well plates and treated with gefitinib (5 μ M) alone, fenofibrate (20, 40 μ M) alone or both drugs. After incubation for 48 h, cells were harvested without EDTA and washed with ice-cold PBS, and an Annexin V-FITC/PI Apoptosis Detection Kit (Vazyme, Nanjing, China) was used following the manufacturer's protocol. After incubation with 5 μ L of Annexin V-FITC and 5 μ L of propidium iodide on ice for 10 min in the dark, the cells were immediately analyzed by FACS on a flow cytometer (MiltenyiBiotec, Germany). During the assay, 1×10^4 cells per sample were collected. The results were analyzed using FlowJo VX software. Three individual experiments were repeated.

Xenografts model

Four-week-old male BALB/c nude mice were obtained from Yangzhou University (Yangzhou, China) and maintained in specific pathogen-free conditions at China Pharmaceutical University. All animal experiments were approved by the Ethics Committee of China Pharmaceutical University. PC-9/GR cells (5×10^6 per mouse) were subcutaneously inoculated into BALB/c nude mice. Tumor sizes were measured with a Vernier caliper and calculated using the following formula: tumor volume (mm^3) = $1/2 \times \text{length} \times \text{width}^2$. When the initial average tumor volume was approximately 100 mm^3 , all the animals were randomly divided into four groups as follows: control (treated with saline), gefitinib (treated with 25 mg/kg gefitinib), fenofibrate (treated with 100 mg/kg fenofibrate), and gefitinib combined with fenofibrate (treated with 25 mg/kg gefitinib and 100 mg/kg fenofibrate). All agents were given once a day via intragastric administration. All animals were sacrificed after 14 days of treatment, and tumor tissues were collected and weighed.

Statistical analysis

All data are expressed as the mean \pm SD from at least three separate experiments. GraphPad Prism 7.0 statistical software (GraphPad San Diego, CA, USA) was used for data analysis. The two-tailed Student's *t*-test was used to reveal statistical significance. One-way ANOVA with Dunnett's test or two-way ANOVA with Bonferroni's multiple comparison was used to compare multiple groups. $P < 0.05$ was considered to indicate a statistically significant difference.

RESULTS

Cholesterol and cholesterol efflux pathways are dysregulated in EGFR-mutant NSCLC cells with gefitinib resistance

We selected the gefitinib-sensitive cell line PC-9 and gefitinib-resistant cell lines PC-9/GR, H1975, H1650, and A549 for the following experiments. The IC₅₀ values of gefitinib in the selected

Table 1. The gefitinib IC₅₀ value of cell lines

Cell line	Treatment	IC ₅₀
PC-9	Gefitinib	27.3 \pm 1.4 nM
PC-9/GR	Gefitinib	25.2 \pm 1.7 μ M
H1975	Gefitinib	32.3 \pm 1.5 μ M
H1650	Gefitinib	17.0 \pm 2.1 μ M
A549	Gefitinib	13.6 \pm 1.2 μ M

NSCLC cell lines are summarized in Table 1. To investigate the relationship between intracellular cholesterol level and gefitinib resistance, we detected the intracellular cholesterol level in PC-9, PC-9/GR, H1975, H1650 and A549 cells. All cholesterol assays were normalized to cell number. The Amplex[®] Red Cholesterol Assay kit for cholesterol quantification showed that the intracellular cholesterol level in the gefitinib-resistant cell lines was significantly higher than that in the sensitive cell line (Fig. 1a). PC-9/GR, H1975, H1650 and A549 cells were exposed to gefitinib for 48 h. The results showed that gefitinib exposure remarkably elevated intracellular cholesterol levels in cell lines with acquired gefitinib resistance (PC-9/GR, H1975, H1650) compared with those in cells treated with vehicle (Fig. 1b); however, this phenomenon did not occur in EGFR wild-type cells (A549). These results demonstrated that elevated intracellular cholesterol levels were a consequence of gefitinib resistance; therefore, eliminating intracellular cholesterol is a potential strategy to relieve gefitinib resistance.

Next, to verify the dysregulation of cholesterol efflux in gefitinib-resistant NSCLC cells, the protein expression of PPAR α , LXRA, and ABCA1 was detected. The results revealed that the protein expression of PPAR α , LXRA, and ABCA1 was significantly decreased in gefitinib-resistant cell lines compared with the gefitinib-sensitive cell line (Fig. 1c). Furthermore, when the gefitinib-resistant cell lines were exposed to a dose of 5 μ M gefitinib for 48 h, the protein expression of PPAR α , LXRA, and ABCA1 was downregulated compared to that in cells treated with vehicle (Fig. 1d). These findings showed that dysregulation of the cholesterol efflux pathway might induce cholesterol accumulation in NSCLC cell lines with acquired gefitinib resistance. Furthermore, gefitinib could enhance the dysregulation of the cholesterol efflux pathway.

Fenofibrate potentiates the gefitinib cytotoxicity in gefitinib-resistant NSCLC cells

Then, we explored how the PPAR α agonist fenofibrate increased gefitinib cytotoxicity in gefitinib-resistant NSCLC cells. As the results revealed, the indicated concentration of fenofibrate could obviously increase the expression of PPAR α , and significantly increased expression of LXRA and ABCA1 occurred at the high concentration (40 μ M) (Fig. 2a). Fenofibrate also reduced the intracellular cholesterol level in a time-dependent manner in gefitinib-resistant cells (Fig. 2b). Then, we investigated the cytotoxicity of various concentrations of fenofibrate in gefitinib-resistant cells, the results suggested that fenofibrate has a slightly antiproliferative effect in gefitinib-resistant cells (Fig. 2c), the inhibition rate of high concentration group (40 μ M) was ~20%. Next, we detected the synergistic effect of gefitinib and fenofibrate in gefitinib-resistant cells. The results revealed that the indicated concentration of fenofibrate with different concentrations of gefitinib prominently increased gefitinib cytotoxicity and reduced the IC₅₀ against gefitinib (Fig. 2d, e). CI values also demonstrated the synergistic interactions of gefitinib and fenofibrate (Table 2). Moreover, the results of colony forming assays suggested that the drug combination reduced the colony formation ability of gefitinib-resistant cells (Fig. 2f, g). All the results indicated that fenofibrate remarkably potentiated gefitinib cytotoxicity in gefitinib-resistant NSCLC cells, and the combination

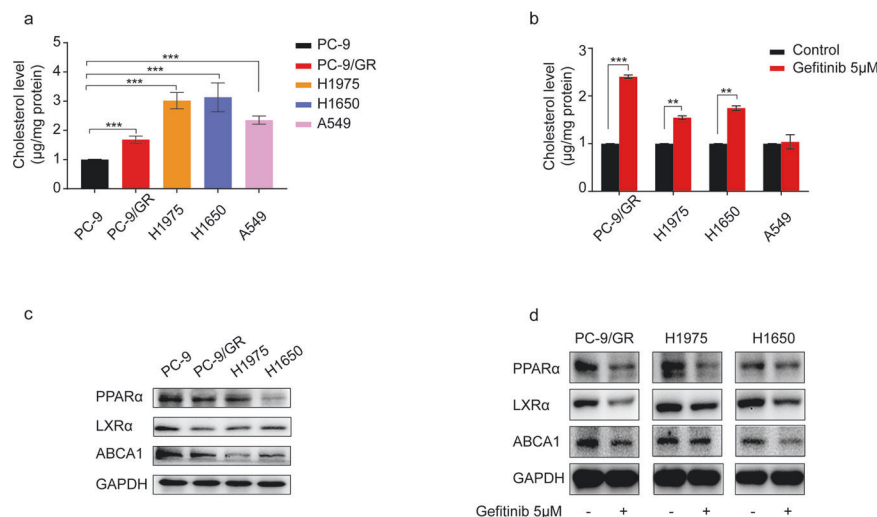


Fig. 1 Intracellular cholesterol levels and cholesterol efflux pathways were dysregulated in gefitinib-resistant NSCLC cell lines. **a** PC-9, PC-9/GR, H1975, H1650, and A549 cells were plated at a density of 2×10^5 cells per well. Cholesterol levels were measured using the Amplex[®] Red Cholesterol Assay Kit. The samples were normalized to protein concentration for a final value in μg cholesterol/mg protein, and the fold change of PC-9 cholesterol/protein level was calculated. Experiments were repeated at least three times in duplicate, and all values are given as the means \pm SDs. Statistical analysis was performed utilizing Student's *t*-test; $***P \leq 0.001$ vs PC-9. **b** PC-9/GR, H1975, H1650, and A549 cells were plated at a density of 2×10^5 cells per well. Cellular cholesterol was measured after gefitinib treatment for 48 h. All values are given as the means \pm SDs, and statistical analysis was performed utilizing Student's *t*-test; $**P \leq 0.01$, $***P \leq 0.001$ vs control. **c** PPAR α , LXR α , and ABCA1 expression was analyzed by Western blot in PC-9, PC-9/GR, H1975, and H1650 cell lines. **d** Western blot analysis of PPAR α , LXR α , and ABCA1 expression after gefitinib (5 μM) treatment for 48 h in PC-9/GR, H1975, and H1650 cell lines

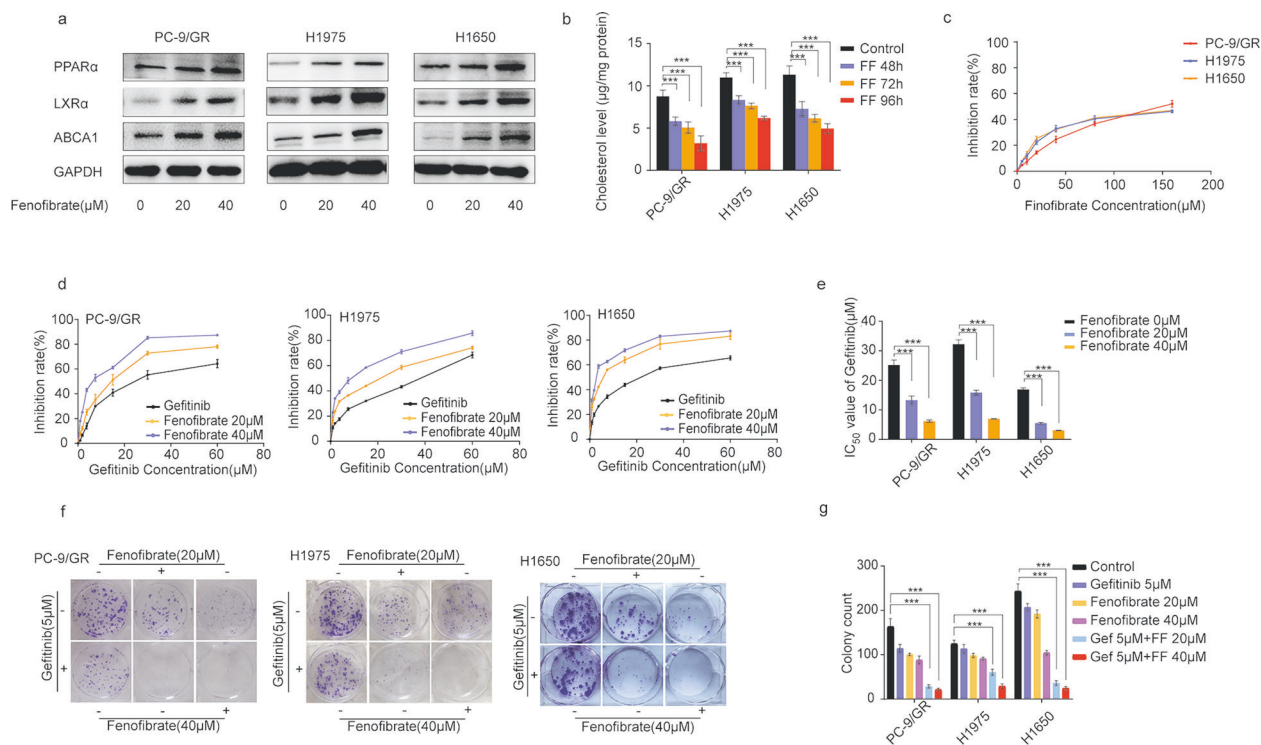


Fig. 2 Fenofibrate enhanced gefitinib cytotoxicity in gefitinib-resistant cells. **a** Western blot analysis of PPAR α , LXR α , and ABCA1 expression after fenofibrate (20 and 40 μM) treatment for 48 h in PC-9/GR, H1975, and H1650 cell lines. **b** Cellular cholesterol was measured after fenofibrate (40 μM) treatment for 48, 72 and 96 h. Statistical analysis was performed utilizing Student's *t*-test; $***P \leq 0.001$ vs control. **c** PC-9/GR, H1975, and H1650 cells were plated at a density of 5000 cells per well. PC-9/GR, H1975, and H1650 cells were treated with various concentrations of fenofibrate (0, 5, 10, 20, 40, 80, and 160 μM) for 48 h, and the CCK-8 assay was used to determine cytotoxicity. **d** Cells were treated with various concentrations of gefitinib (0.9375, 1.875, 3.75, 7.5, 15, 30, and 60 μM) combined with fenofibrate (20, 40 μM) for 48 h, and a CCK-8 assay was used to determine cytotoxicity. **e** The IC_{50} values of gefitinib were analyzed when gefitinib was combined with fenofibrate. Statistical analysis was performed utilizing Student's *t*-test; $***P \leq 0.001$ vs control. **f** and **g** The colony formation assay of PC-9/GR, H1975, and H1650 cells was analyzed when gefitinib (5 μM) was combined with fenofibrate (20, 40 μM). All values are presented as the means \pm SDs. Statistical analysis was performed utilizing Student's *t*-test; $***P \leq 0.001$ vs control

Table 2. The combination index (CI) of fenofibrate and gefitinib in gefitinib-resistant cell lines

Dose gefitinib (μM)	Dose fenofibrate (μM)	CI
PC-9/GR		
0.9375	20	0.73
1.875	20	0.57
3.75	20	0.35
7.5	20	0.24
15	20	0.24
30	20	0.22
60	20	0.28
0.9375	40	0.66
1.875	40	0.52
3.75	40	0.35
7.5	40	0.24
15	40	0.17
30	40	0.13
60	40	0.20
H1975		
0.9375	20	0.89
1.875	20	0.47
3.75	20	0.39
7.5	20	0.35
15	20	0.28
30	20	0.19
60	20	0.12
0.9375	40	0.87
1.875	40	0.47
3.75	40	0.42
7.5	40	0.37
15	40	0.25
30	40	0.16
60	40	0.19
H1650		
0.9375	20	0.94
1.875	20	0.90
3.75	20	0.44
7.5	20	0.38
15	20	0.22
30	20	0.21
60	20	0.24
0.9375	40	0.71
1.875	40	0.53
3.75	40	0.27
7.5	40	0.25
15	40	0.26
30	40	0.13
60	40	0.13

fenofibrate single-treatment groups were not dramatically enhanced compared with that of the control group, but the combined treatment comprising fenofibrate and gefitinib significantly increased apoptosis (Fig. 3a–d). Furthermore, key proteins of the intrinsic apoptotic pathway were detected after combination treatment. Our observation indicated that treatment with either fenofibrate alone or gefitinib alone could not significantly initiate the intrinsic apoptotic pathway, and the expression of Bcl-2, Bax, Caspase 3, Caspase 7, Caspase 8, and Caspase 9 was not remarkably changed compared with that in the control group. However, combination treatment of fenofibrate and gefitinib could downregulate the expression of Bcl-2, Caspase 3, Caspase 7, Caspase 8, and Caspase 9 while upregulating the levels of Bax, Cl-Caspase 3, Cl-Caspase 7, Cl-Caspase 8 and Cl-Caspase 9 in gefitinib-resistant cells (Fig. 3e). These results demonstrated that fenofibrate remarkably initiates the intrinsic apoptotic pathway induced by gefitinib. This phenomenon might be one of the mechanisms by which fenofibrate relieves gefitinib resistance in NSCLC cells.

Knockdown of PPAR α diminishes the synergistic effects of fenofibrate and gefitinib

To confirm that fenofibrate could increase gefitinib sensitivity in a PPAR α -dependent manner, siRNA (small interfering RNA) was used to silence PPAR α expression. The results showed that the PPAR α transcript levels were remarkably decreased after transfection with PPAR α siRNA in PC-9/GR, H1975 and H1650 cells (Fig. 4a). The intracellular cholesterol level was not decreased by fenofibrate after transfection with siPPAR α compared with siNC (Fig. 4b). The synergistic antiproliferative effect of gefitinib and fenofibrate after knockingdown PPAR α was also detected. The results showed that fenofibrate did not increase gefitinib sensitivity when PPAR α was silenced (Fig. 4c, d). The results of colony forming assays showed the same trend (Fig. 4e, f). All these data revealed that the synergistic effects of fenofibrate and gefitinib occur in a PPAR α -dependent manner.

Fenofibrate resensitizes gefitinib treatment via the AMPK/AKT/FoxO1 pathway in a PPAR α -dependent manner

Next, we investigated the antiproliferative mechanism and the promotion of apoptosis induced by fenofibrate combined with gefitinib. The protein expression levels of PPAR α , AMPK, p-AMPK, AKT, p-AKT, FoxO1 and p-FoxO1 were detected in cells treated with the indicated concentrations of fenofibrate and gefitinib alone or in combination. The results revealed that gefitinib decreased the protein expression of PPAR α but had no significant effect on the expression of other proteins. Conversely, fenofibrate decreased the protein expression of p-FoxO1 and increased the protein expression of AMPK, p-AMPK, and FoxO1 compared to that of cells treated with vehicle. Combined use of fenofibrate with gefitinib increased the protein expression of AMPK, p-AMPK, and FoxO1 and decreased the protein expression of AKT, p-AKT, and p-FoxO1 by activating PPAR α compared with that observed after treatment with vehicle or gefitinib alone (Fig. 5a). Then, siRNA targeting AMPK was used in this study, and we found that after transfecting siAMPK, AMPK, p-AMPK and FOXO1 expression in NSCLC cell lines was remarkably inhibited, while p-FOXO1 and p-AKT levels were upregulated. Moreover, siAMPK and fenofibrate in combination with gefitinib effectively reversed the expression of AMPK, p-AMPK, AKT, p-AKT, FOXO1 and p-FOXO1. These data indicated that the effect of the combination of gefitinib and fenofibrate on regulating AKT and FOXO1 expression was associated with AMPK (Fig. 5b). SC79, an AKT agonist, could activate the AKT pathway by upregulating p-AKT levels. The results showed that SC79 could upregulate p-AKT and p-FOXO1 while downregulating FOXO1. Fenofibrate combined with gefitinib remarkably reversed the regulation of p-AKT, FOXO1 and p-FOXO1 induced by SC79. These data proved that the effects of

of fenofibrate and gefitinib might be a promising strategy to relieve gefitinib resistance.

Fenofibrate potentiates gefitinib sensitivity by modulating apoptosis

Whether fenofibrate increases gefitinib cytotoxicity by inducing apoptosis was confirmed. The apoptosis rates of the gefitinib and

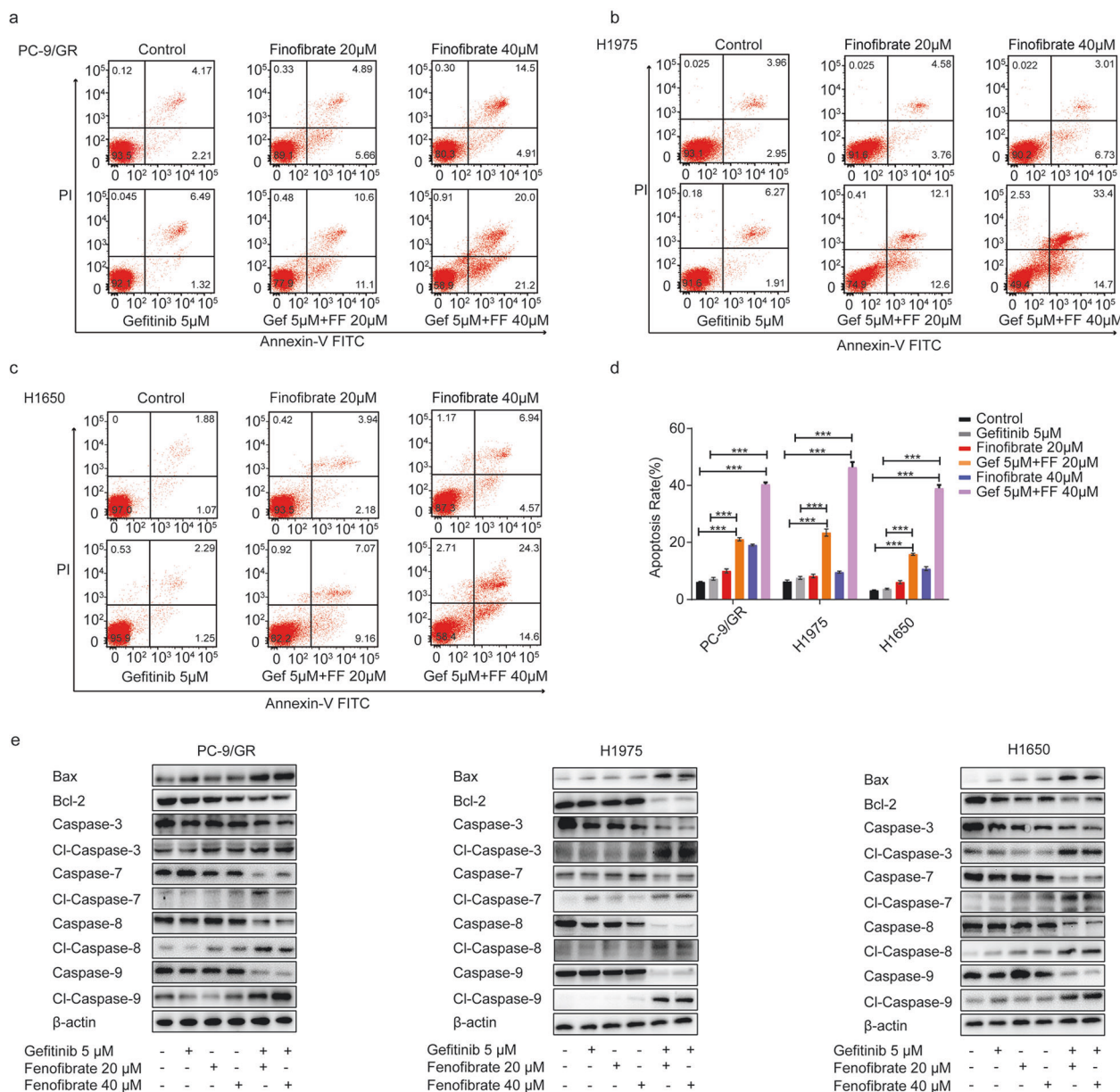


Fig. 3 Fenofibrate potentiated gefitinib-induced apoptosis. **a**, **b**, and **c** PC-9/GR, H1975, and H1650 cells were plated at a density of 2×10^5 cells per well and treated with gefitinib (5 μ M) alone, fenofibrate (20, 40 μ M) or both for 48 h. Apoptosis was analyzed by flow cytometry with Annexin V/PI staining. **d** Apoptosis rates are shown in the bar graph. All values are given as the means \pm SDs, and statistical analysis was performed utilizing Student's *t*-test; $***P \leq 0.001$ vs the control or gefitinib group. **e** Western blot analysis for Bax, Bcl-2, Caspase-3, Cl-Caspase-3, Caspase-7, Cl-Caspase-7, Caspase-8, Cl-Caspase-8, Caspase-9, Cl-Caspase-9 protein expression in PC-9/GR, H1975, and H1650 cells treated with gefitinib (5 μ M) alone, fenofibrate (20, 40 μ M) alone or both drugs for 48 h

the combination of gefitinib and fenofibrate on regulating FOXO1 were correlated with the AMPK/AKT axis (Fig. 5c). Furthermore, PPAR α knockdown reversed the effect mediated by the combined use of fenofibrate and gefitinib. The results showed that compared with the negative control (siNC), PPAR α knockdown (siPPAR α) slightly influenced the AMPK/AKT/FoxO1 signaling pathway. However, PPAR α knockdown (siPPAR α) remarkably weakened the effects of fenofibrate on the AMPK/AKT/FoxO1 signaling pathway. Moreover, after knockdown of PPAR α in NSCLC cell lines, fenofibrate combined with gefitinib effectively reversed the protein expression of the AMPK/AKT/FoxO1 signaling pathway compared with that in cells without siPPAR α treatment (Fig. 5d). These data proved that fenofibrate potentiated gefitinib sensitivity by regulating the AMPK/AKT/FoxO1 pathway in a PPAR α -dependent manner.

Combined treatment of gefitinib with fenofibrate inhibits NSCLC progression in vivo

Based on the above results, we further evaluated whether fenofibrate could increase gefitinib sensitivity in a xenograft mouse model. We used PC-9/GR cell lines to establish a xenograft mouse model and evaluated the antitumor effect of gefitinib and fenofibrate either alone or in combination. The results indicated that none of the treatments significantly influenced the weights of nude mice (Fig. 6a). As expected, the gefitinib and fenofibrate monotherapies exhibited no significant antitumor effect in nude mice, but the combination treatment remarkably suppressed the tumor volume and tumor weight compared with those after either single treatment (Fig. 6b–d). These data were consistent with the in vitro results and revealed that fenofibrate could increase the sensitivity of gefitinib in vivo.

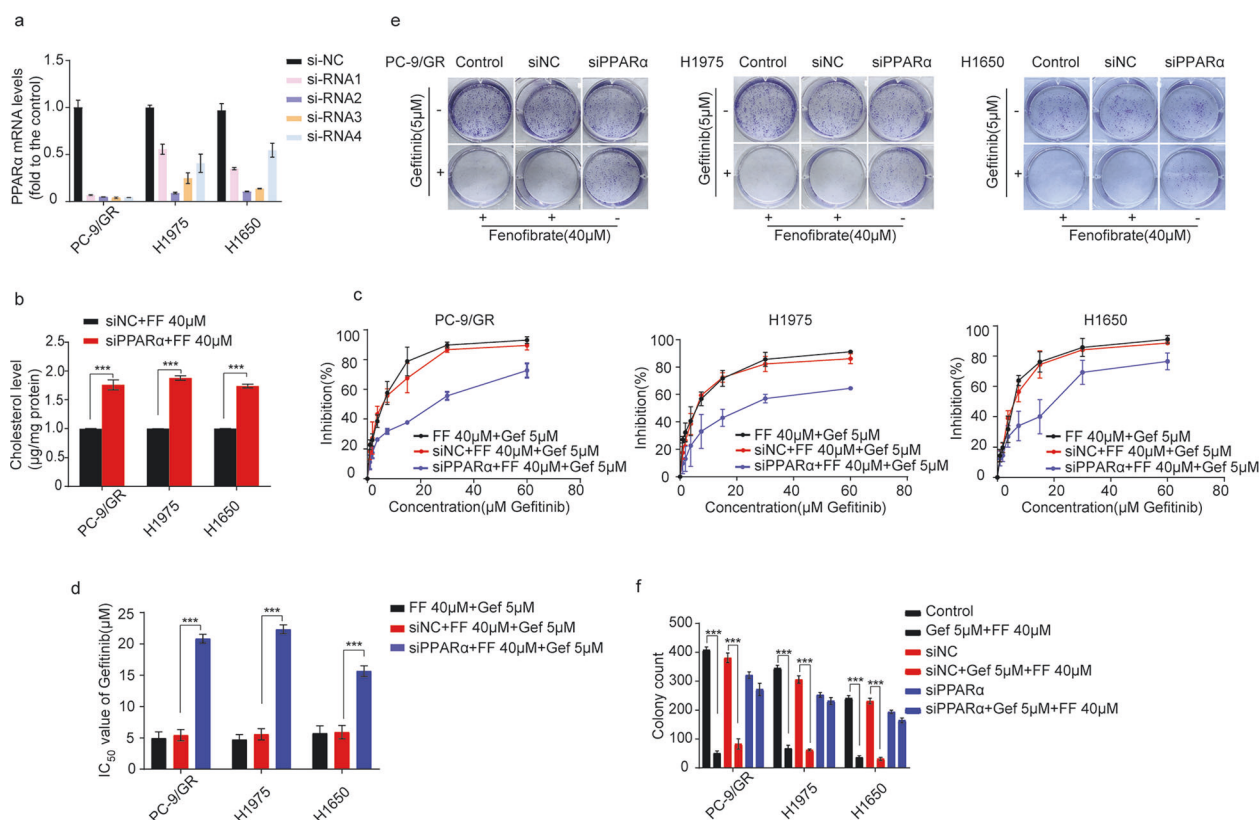


Fig. 4 Silencing PPARα diminished the synergistic effect of fenofibrate and gefitinib. **a** PPARα mRNA levels in PC-9/GR, H1975, and H1650 cells were tested by RT-PCR after transfection with siRNA targeting PPARα. **b** siRNA was transfected, and after 6 h, fenofibrate (40 μM) was added for 48 h. The cellular cholesterol level was measured as described above. Statistical analysis was performed utilizing Student's *t*-test; ****P* ≤ 0.001 vs the siNC plus fenofibrate group. **c** and **d** siNC and siPPARα were transfected into PC-9/GR, H1975, and H1650 cells. After 6 h, various concentrations of gefitinib (0.9375, 1.875, 3.75, 7.5, 15, 30, and 60 μM) were added in combination with fenofibrate (20, 40 μM) treatment for 48 h. The CCK-8 assay was used to determine the cytotoxicity and IC₅₀ values. All values are given as the means ± SDs, and statistical analysis was performed utilizing Student's *t*-test; ****P* ≤ 0.001 vs the siNC plus fenofibrate and gefitinib treatment group. **e** and **f** siNC and siPPARα were transfected into PC-9/GR, H1975, and H1650 cells. The colony formation assay of PC-9/GR, H1975, and H1650 cells was analyzed when gefitinib (5 μM) and fenofibrate (40 μM) were coadministered. All values are given as the means ± SDs. Statistical analysis was performed utilizing Student's *t*-test; ****P* ≤ 0.001 vs control or siNC

DISCUSSION

Gefitinib, an EGFR tyrosine kinase inhibitor, shows a highly specific affinity for EGFR and significantly affects the survival of NSCLC patients harboring EGFR mutations [21]. Despite many patients exhibiting an initial response to gefitinib, acquired drug resistance is the major reason for the failure of gefitinib treatment in NSCLC patients harboring EGFR mutations, with a median time to disease progression of approximately 10–12 months [21]. Recent research indicates that high cholesterol levels in lipid rafts may contribute to gefitinib resistance in NSCLC cell lines [10]; however, the mechanism by which high cholesterol influences gefitinib resistance is not clear. We revealed the phenomenon of high intracellular cholesterol levels in gefitinib-resistant cell lines and found that PPARα/LXRα/ABCA1 axis, which are constituents of the cholesterol efflux pathway, was downregulated and influenced the intracellular cholesterol level after gefitinib treatment. Furthermore, we first proposed that the combination of the PPARα agonist fenofibrate and gefitinib overcomes gefitinib resistance. This therapeutic option provides a new strategy to enhance gefitinib cytotoxicity.

A great deal of evidence indicates that cholesterol utilization by malignant cancer cells is a crucial feature of carcinogenesis and that cholesterol metabolism has a close relationship with the development of tumorigenesis and drug resistance [22]. Recent studies have shown that increased serum cholesterol levels correlate with a high risk of developing cancers, such as prostate,

colon and rectal cancer [23]. In our study, we discovered that the intracellular cholesterol level in gefitinib-resistant cells was higher than that in gefitinib-sensitive cells. Furthermore, when the drug-resistant cell lines were exposed to gefitinib, the level of intracellular cholesterol was further elevated, which was consistent with previous reports [8, 10]. This revealed that the deregulation of cholesterol homeostasis is an important contributing factor to gefitinib resistance in NSCLC cells.

In cancer cells, cholesterol homeostasis is regulated by a complex protein network that involves cholesterol synthesis, import, export, metabolism and esterification [24]. Sterol-regulatory element binding protein transcription factor 2 and liver X receptors (LXRs) are the key regulators of cholesterol homeostasis in cancer cells [25]. In the cholesterol synthesis pathway, the activity of the key protein HMGCR is enhanced by both the transcriptional regulation of SREBP and changes in the feedback control of HMGCR [26]. Low-density lipoprotein (LDL) particles transport cholesterol to most surrounding tissues, and activation of SREBP could regulate the LDL receptor to promote cholesterol influx [26]. When cholesterol accumulates in cancer cells, the increased intracellular cholesterol level shuts down cholesterol synthesis and promotes cholesterol export [27]. Our study focused on the deregulation of the PPARα/LXRα/ABCA1 cholesterol export pathway in gefitinib-resistant cell lines and discovered that the expression of PPARα, LXRα, and ABCA1 were significantly decreased in gefitinib-resistant cell lines

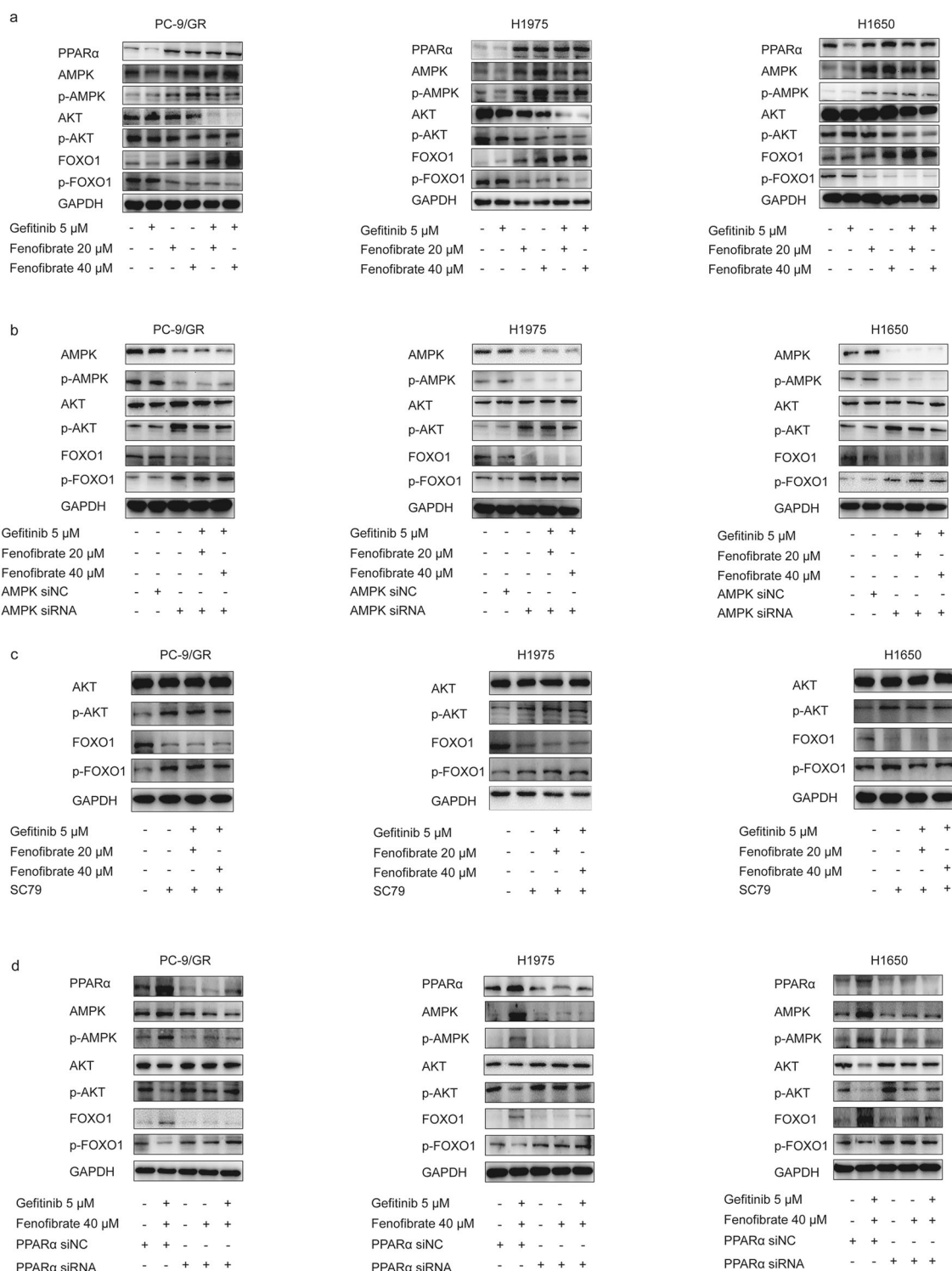


Fig. 5 Fenofibrate resensitized gefitinib treatment via the AMPK/AKT/FoxO1 pathway in a PPARα-dependent manner. **a** Western blot analysis of PPARα, AMPK, p-AMPK, AKT, p-AKT, FoxO1, and p-FoxO1 expression in PC-9/GR, H1975, and H1650 cells treated with gefitinib (5 μM), fenofibrate (20, 40 μM) or both drugs for 48 h. **b** siNC and siAMPK were transfected into PC-9/GR, H1975, and H1650 cells after 6 h before cells were treated with gefitinib (5 μM) and fenofibrate (20, 40 μM) for 48 h. Western blot analysis for AMPK, p-AMPK, AKT, p-AKT, FoxO1, and p-FoxO1 expression. **c** Western blot analysis for AKT, p-AKT, FoxO1, and p-FoxO1 expression in PC-9/GR, H1975, and H1650 cells treated with SC79 (1 μM) alone or in combination with other drugs for 48 h. **d** siNC and siPPARα were transfected into PC-9/GR, H1975, and H1650 cells after 6 h before cells were treated with fenofibrate (20, 40 μM) alone or in combination with other drugs for 48 h

compared with gefitinib-sensitive cell lines. Moreover, the expression of PPARα, LXRA, and ABCA1 was persistently decreased during gefitinib treatment in drug-resistant cell lines. These results proved that the PPARα/LXRα/ABCA1

cholesterol export pathway might be a potential target to overcome gefitinib resistance in NSCLC cells and that the combined use of a PPARα agonist with gefitinib could increase gefitinib cytotoxicity.

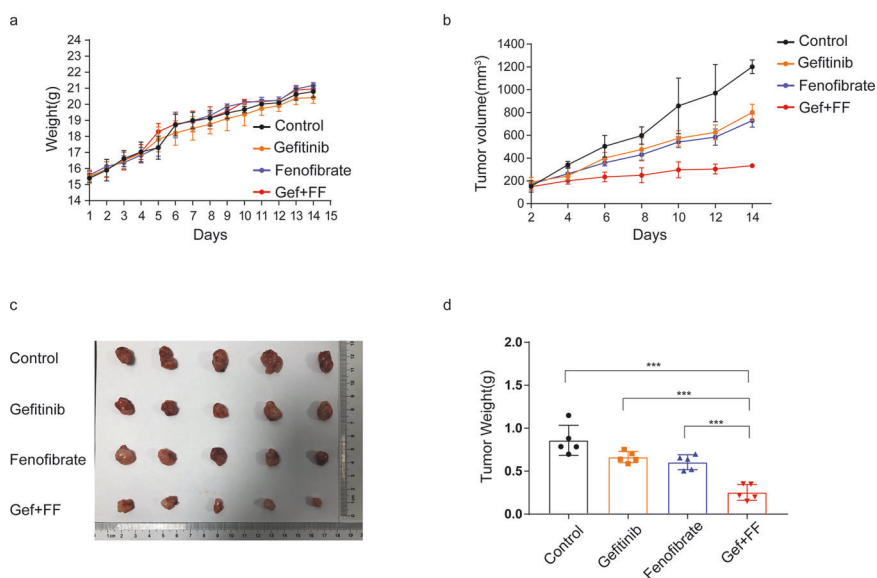


Fig. 6 Fenofibrate increased gefitinib cytotoxicity in a xenograft mouse model. **a** and **b** Body weight and tumor sizes of nude mice are presented in a line graph. **c** Macroscopic appearance of xenografts from each group ($n = 5$). **d** Tumor weight is presented as the mean \pm SD, and statistical analysis was performed utilizing Student's t -test; $***P \leq 0.001$ vs control

Next, we detected the effect of the combined use of the PPAR α agonist fenofibrate with gefitinib on gefitinib-resistant cells. Fenofibrate, a potent agonist of PPAR α , has been a widely used lipid-lowering drug in the clinic since its introduction in 1975 [28]. In recent years, some studies have revealed that fenofibrate could significantly lower total mortality and reduce the rate of cancer-related death [29, 30]. A series of studies showed that fenofibrate displays antiproliferative effects in lung cancer, breast cancer, gastric cancer, prostate cancer and glioma [29, 31–34], and further research revealed that fenofibrate could potentiate chemosensitivity effects in human breast cancer cells [35]. However, whether the antitumor effect of fenofibrate is dependent on PPAR α remains controversial. Our study used a series of experiments to reveal that fenofibrate could increase the cytotoxicity of gefitinib in drug-resistant cell lines in a PPAR α -dependent manner. In the cell viability assay, we confirmed that the antiproliferative effects of gefitinib on drug-resistant cell lines were strengthened by fenofibrate treatment in a dose-dependent manner. However, there was no significant inhibition in NSCLC cell lines when cells were treated with fenofibrate alone. The colony formation assay also supported our conclusions above. We further proved that fenofibrate increased the sensitivity to gefitinib in a PPAR α -dependent manner. From our observations, the antiproliferative effects that were increased by fenofibrate were abrogated when PPAR α was silenced. The same conclusions could be drawn by the colony formation assay. These results provided evidence that fenofibrate increased gefitinib cytotoxicity in gefitinib-resistant NSCLC cell lines via activation of PPAR α .

What is the detailed mechanism by which fenofibrate increases gefitinib cytotoxicity in NSCLC cell lines? Previous studies reported that fenofibrate could potentiate the chemosensitivity of cancer cells by modulating apoptosis. Fenofibrate dramatically enhanced paclitaxel-induced apoptosis in breast cancer cells and increased the expression of intrinsic apoptotic pathway proteins [35]. In our study, we discovered that fenofibrate could significantly enhance gefitinib-induced apoptosis in drug-resistant cell lines, while fenofibrate alone did not increase apoptosis. Moreover, the levels of intrinsic apoptotic pathway proteins Bcl-2, Caspase 3, Caspase 7, Caspase 8, Caspase 9 remarkably decreased and the levels of Bax, Cl-Caspase 3, Cl-Caspase 7, Cl-Caspase 8, Cl-Caspase 9 increased in cells treated with fenofibrate plus gefitinib. Our results indicated that fenofibrate could enhance cellular sensitivity to gefitinib by

activating the intrinsic apoptotic pathway in vitro. Then, we investigated whether fenofibrate enhanced gefitinib-induced apoptosis via activation of the PPAR α /AMPK/AKT/FoxO1 pathway. It is well known that the AMPK/AKT/FoxO1 pathway is the key regulator of cell proliferation, survival and apoptosis [36]. AMPK is an energy sensor protein that is considered a molecular target for lipid metabolism. Activation of PPAR α could induce transcriptional activation of fatty acid β -oxidation machinery and switch energy metabolism from glucose to fatty acid utilization, both of which result in decreased ATP levels and increased activated AMPK levels [36]. A study reported that the activation of PPAR α could increase AMPK phosphorylation and consequently regulate FOXO1 expression and localization [37]. According to published evidence, we investigated whether fenofibrate acts on the PPAR α /AMPK/AKT/FoxO1 pathway to increase gefitinib cytotoxicity. As expected, the results demonstrated that fenofibrate activated PPAR α and increased the phosphorylation of AMPK. Activated AMPK suppressed AKT expression and phosphorylation and stimulated FoxO1 expression to activate intrinsic apoptosis. The above phenomenon was abrogated when we knocked down PPAR α , indicating that fenofibrate influenced the AMPK/AKT/FoxO1 pathway to promote gefitinib-induced apoptosis in a PPAR α -dependent manner.

In summary, this study propose that the PPAR α agonist fenofibrate could relieve gefitinib resistance in NSCLC cell lines by regulating the PPAR α /AMPK/AKT/FoxO1 signaling pathway. This study aimed to find a promising strategy to overcome gefitinib resistance in NSCLC and provide a theoretical basis for clinical application.

ACKNOWLEDGEMENTS

We thank molecular Experiment Platform of Stat Key Laboratory of Natural Medicines at China Pharmaceutical University for providing Flow Cytometry.

AUTHOR CONTRIBUTIONS

MSW, QSH, and ZRJ designed the research methods, performed the experiments, and prepared the manuscript. MSW analyzed the data. CSC, QQL, YMZ, KWW, JW, KX, and CQ participated in experiments. XSD conceived the projects, designed, and revised the manuscript. All authors read and approved the final manuscript.

ADDITIONAL INFORMATION

Competing interests: The authors declare no competing interests.

REFERENCES

- Bray F, Ferlay J, Soerjomataram I, Siegel RL, Torre LA, Jemal A. Global cancer statistics 2018: GLOBOCAN estimates of incidence and mortality worldwide for 36 cancers in 185 countries. *CA Cancer J Clin.* 2018;68:394–424.
- Herbst RS, Morgensztern D, Boshoff C. The biology and management of non-small cell lung cancer. *Nature.* 2018;553:446–54.
- Ettinger DS, Aisner DL, Wood DE, Akerley W, Bauman J, Chang JY, et al. NCCN guidelines insights: non-small cell lung cancer, version 5.2018. *J Natl Compr Canc Netw.* 2018;16:807–21.
- Kosaka T, Yatabe Y, Endoh H, Yoshida K, Hida T, Tsuboi M, et al. Analysis of epidermal growth factor receptor gene mutation in patients with non-small cell lung cancer and acquired resistance to gefitinib. *Clin Cancer Res.* 2006;12:5764–9.
- Rocco D, Battiloro C, Gravara LD, Gridelli C. Advanced non-small cell lung cancer with activating epidermal growth factor receptor mutation: first line treatment and beyond. *Rev Recent Clin Trials.* 2019;14:120–8.
- Wu SG, Shih JY. Management of acquired resistance to EGFR TKI-targeted therapy in advanced non-small cell lung cancer. *Mol Cancer.* 2018;17:38.
- Hirsch HA, Iliopoulos D, Joshi A, Zhang Y, Jaeger SA, Bulyk M, et al. A transcriptional signature and common gene networks link cancer with lipid metabolism and diverse human diseases. *Cancer Cell.* 2010;17:348–61.
- Ali A, Levantini E, Fhu CW, Teo JT, Clohessy JG, Goggi JL, et al. CAV1–GLUT3 signaling is important for cellular energy and can be targeted by atorvastatin in non-small cell lung cancer. *Theranostics.* 2019;9:6157–74.
- Ercan D, Choi HG, Yun CH, Capelletti M, Xie T, Eck MJ, et al. EGFR mutations and resistance to irreversible pyrimidine-based EGFR inhibitors. *Clin Cancer Res.* 2015;21:3913–23.
- Chen Q, Pan Z, Zhao M, Wang Q, Qiao C, Miao L, et al. High cholesterol in lipid rafts reduces the sensitivity to EGFR-TKI therapy in non-small cell lung cancer. *J Cell Physiol.* 2018;233:6722–32.
- Ali A, Levantini E, Teo JT, Goggi J, Clohessy JG, Wu CS, et al. Fatty acid synthase mediates EGFR palmitoylation in EGFR mutated non-small cell lung cancer. *EMBO Mol Med.* 2018;10:e8313.
- Smith B, Land H. Anticancer activity of the cholesterol exporter ABCA1 gene. *Cell Rep.* 2012;2:580–90.
- Sharma B, Agnihotri N. Role of cholesterol homeostasis and its efflux pathways in cancer progression. *J Steroid Biochem Mol Biol.* 2019;191:105377.
- Pawlak M, Lefebvre P, Staels B. Molecular mechanism of PPAR α action and its impact on lipid metabolism, inflammation and fibrosis in non-alcoholic fatty liver disease. *J Hepatol.* 2015;62:720–33.
- Ogata M, Tsujita M, Hossain MA, Akita N, Gonzalez FJ, Staels B, et al. On the mechanism for PPAR agonists to enhance ABCA1 gene expression. *Atherosclerosis.* 2009;205:413–9.
- Xu N, Wang Q, Jiang S, Wang Q, Hu W, Zhou S, et al. Fenofibrate improves vascular endothelial function and contractility in diabetic mice. *Redox Biol.* 2019;20:87–97.
- Desvergne B, Wahli W. Peroxisome proliferator-activated receptors: nuclear control of metabolism. *Endocr Rev.* 1999;20:649–88.
- Lian X, Wang G, Zhou H, Zheng Z, Fu Y, Cai L. Anticancer properties of fenofibrate: a repurposing use. *J Cancer.* 2018;9:1527–37.
- Sun J, Zheng Z, Chen Q, Pan Y, Quan M, Dai Y. Fenofibrate potentiates chemosensitivity to human breast cancer cells by modulating apoptosis via AKT/NF- κ B pathway. *Onco Targets Ther.* 2019;12:773–83.
- Luty M, Piwowarczyk K, Labedz-Maslowska A, Wrobel T, Szczygiel M, Catapano J, et al. Fenofibrate augments the sensitivity of drug-resistant prostate cancer cells to docetaxel. *Cancers (Basel).* 2019;11:77.
- Sirotnak FM, Zakowski MF, Miller VA, Scher HI, Kris MG. Efficacy of cytotoxic agents against human tumor xenografts is markedly enhanced by coadministration of ZD1839 (Iressa), an inhibitor of EGFR tyrosine kinase. *Clin Cancer Res.* 2000;6:4885–92.
- Ding X, Zhang W, Li S, Yang H. The role of cholesterol metabolism in cancer. *Am J Cancer Res.* 2019;9:219–27.
- Mabuchi H, Kita T, Matsuzaki M, Matsuzawa Y, Nakaya N, Oikawa S, et al. Large-scale cohort study of the relationship between serum cholesterol concentration and coronary events with low-dose simvastatin therapy in Japanese patients with hypercholesterolemia and coronary heart disease: secondary prevention cohort study of the Japan Lipid Intervention Trial (J-LIT). *Circ J.* 2002;66:1096–100.
- Ikonen E. Cellular cholesterol trafficking and compartmentalization. *Nat Rev Mol Cell Biol.* 2008;9:125–38.
- Kuzu OF, Noory MA, Robertson GP. The role of cholesterol in cancer. *Cancer Res.* 2016;76:2063–70.
- Gobel A, Breining D, Rauner M, Hofbauer LC, Rachner TD. Induction of 3-hydroxy-3-methylglutaryl-CoA reductase mediates statin resistance in breast cancer cells. *Cell Death Dis.* 2019;10:91.
- Villa GR, Hulce JJ, Zanca C, Bi J, Ikegami S, Cahill GL, et al. An LXR-cholesterol axis creates a metabolic co-dependency for brain cancers. *Cancer Cell.* 2016;30:683–93.
- Staels B, Dallongeville J, Auwerx J, Schoonjans K, Leitersdorf E, Fruchart JC. Mechanism of action of fibrates on lipid and lipoprotein metabolism. *Circulation.* 1998;98:2088–93.
- Chen L, Peng J, Wang Y, Jiang H, Wang W, Dai J, et al. Fenofibrate-induced mitochondrial dysfunction and metabolic reprogramming reversal: the anti-tumor effects in gastric carcinoma cells mediated by the PPAR pathway. *Am J Transl Res.* 2020;12:428–46.
- Gardette V, Bongard V, Dallongeville J, Arveiler D, Bingham A, Ruidavets JB, et al. Ten-year all-cause mortality in presumably healthy subjects on lipid-lowering drugs (from the Prospective Epidemiological Study of Myocardial Infarction [PRIME] prospective cohort). *Am J Cardiol.* 2009;103:381–6.
- Goncalves MD, Hwang SK, Pauli C, Murphy CJ, Cheng Z, Hopkins BD, et al. Fenofibrate prevents skeletal muscle loss in mice with lung cancer. *Proc Natl Acad Sci USA.* 2018;115:E743–52.
- Li T, Zhang Q, Zhang J, Yang G, Shao Z, Luo J, et al. Fenofibrate induces apoptosis of triple-negative breast cancer cells via activation of NF- κ B pathway. *BMC Cancer.* 2014;14:96.
- Zhao H, Zhu C, Qin C, Tao T, Li J, Cheng G, et al. Fenofibrate down-regulates the expressions of androgen receptor (AR) and AR target genes and induces oxidative stress in the prostate cancer cell line LNCaP. *Biochem Biophys Res Commun.* 2013;432:320–5.
- Binello E, Mormone E, Emdad L, Kothari H, Germano IM. Characterization of fenofibrate-mediated anti-proliferative pro-apoptotic effects on high-grade gliomas and anti-invasive effects on glioma stem cells. *J Neurooncol.* 2014;117:225–34.
- Sun J, Zheng Z, Chen Q, Pan Y, Quan M, Dai Y. Fenofibrate potentiates chemosensitivity to human breast cancer cells by modulating apoptosis via AKT/NF- κ B pathway. *Oncol Targets Ther.* 2019;12:773–83.
- Zou J, Hong L, Luo C, Li Z, Zhu Y, Huang T, et al. Metformin inhibits estrogen-dependent endometrial cancer cell growth by activating the AMPK-FOXO1 signal pathway. *Cancer Sci.* 2016;107:1806–17.
- Chen WL, Chen YL, Chiang YM, Wang SG, Lee HM. Fenofibrate lowers lipid accumulation in myotubes by modulating the PPAR α /AMPK/FoxO1/ATGL pathway. *Biochem Pharmacol.* 2012;84:522–31.